

# ARES+MOOG - a practical overview of an EW method to derive stellar parameters

Sérgio G. Sousa

**Abstract** The goal of this document is to describe the important practical aspects in the use of an Equivalent Width (EW) method for the derivation of spectroscopic stellar parameters. A general description of the fundamental steps composing any EW method is given, together with possible differences that may be found in different methods used in the literature. Then ARES+MOOG is then used as an example where each step of the method is described in detail. A special focus is given for the specific steps of this method, namely the use of a differential analysis to define the atomic data for the adopted line list, the automatic EW determinations, and the way to find the best parameters at the end of the procedure. Finally, a practical tutorial is given, where we focus on simple exercises useful to illustrate and explain the dependence of the abundances with the assumed stellar parameters. The interdependences are described and a clear procedure is given to find the “final” stellar parameters.

## 1 Introduction

For the derivation of spectroscopic stellar parameters people normally choose between two possible methods. One is normally referred as the “spectral synthesis method”, the other is referred as the “Equivalent Width (EW) method”. The spectral synthesis method typically starts with the synthesis of theoretical spectra which are then compared to the observed spectrum. In this case the “final” parameters are found when the correspondent synthetic spectrum fits the observational spectrum. Alternatively, the EW method starts directly with the observed spectrum, measuring the strength of selected and well-defined absorption lines which are translated into individual line abundances, assuming a given atmospheric model. Then, a compari-

---

Sérgio G. Sousa

Centro de Astrofísica, Universidade do Porto, Rua das Estrelas, 4150-762 Porto and Departamento de Física e Astronomia, Faculdade de Ciências, Universidade do Porto, Rua do Campo Alegre, 4169-007 Porto, Portugal, e-mail: sousasag@astro.up.pt

son between the computed abundances and the respective theoretical predictions is performed in order to find the “final” parameters.

It is clear that both approaches have their own advantages and disadvantages. From one side, the EW method can be faster than the synthetic method since it is focused on only a specific number of lines, while the synthetic method needs a more complete description of the spectrum. On the other hand, if the individual lines used by the EW method cannot be properly isolated then this may lead to inaccurate results.

The goal of this document is to give a description of the “ARES+MOOG method” which is based on the EWs. ARES is the code for automatic EW measurements of the observed spectrum (see Sousa et al. , 2007), and MOOG is used to perform the individual abundance calculations (see Sneden , 1973). The method ARES+MOOG, like other EW methods, allows us to derive the stellar atmospheric parameters: effective temperature ( $T_{\text{eff}}$ ), surface gravity ( $\log g$ ), microturbulence ( $\xi$ ), and the iron abundance ( $[\text{Fe}/\text{H}]$ ). The method makes use of the excitation and ionization balance from the iron lines where the  $[\text{Fe}/\text{H}]$  is used as a proxy for metallicity. This method has been successfully applied to several large samples of F, G, and K (FGK) solar type stars (see e.g. Sousa et al. , 2008, 2011).

## 2 EW Method: a General Overview

Figure 1 reports the workflow describing, as an example of the EW method, the ARES+MOOG procedure to derive the stellar atmospheric parameters. From this diagram we can easily identify the general steps for an EW method based on the excitation and ionization balance of iron lines:

1. A list of iron absorption lines with the correspondent atomic data is selected for the analysis;
2. The observational spectrum is analysed and the EWs are measured independently in a line-by-line analysis;
3. A stellar atmospheric model is adopted given the atmospheric parameters;
4. The measured EWs and the atmospheric models are used to compute the individual line abundances;
5. The “final” spectroscopic parameters are found once the excitation and ionization balance is achieved for all the individual lines analyzed, otherwise we go back to step 3 and adopt different parameters;

These are the basic steps required for the use of an EW method. The differences between the EW methods found in the literature are typically centered on the use of different line lists, models and codes used in each step.

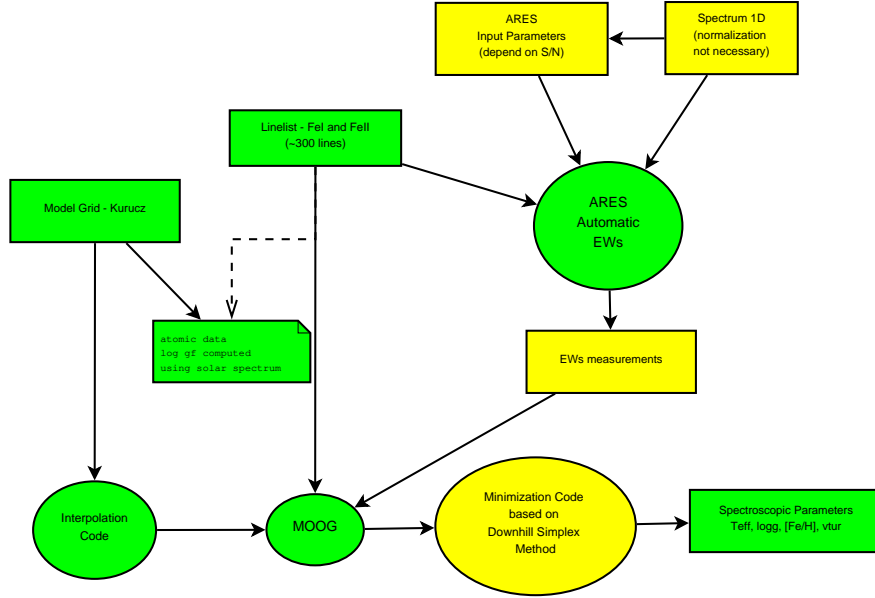


Fig. 1 The workflow diagram of the ARES+MOOG method.

## 2.1 Line-list

The selection of the lines to be used in the analysis (first step) is crucial for the accuracy and precision of this method. **Some authors use a large set of lines** with the aim to increase the statistical strength of the derived spectroscopic stellar parameters. **Others authors use a reduced and very well-defined set of absorption lines** which are considered to be well known or, at least, very well adapted for a specific type of stars (e.g. giant stars).

Together with the line selection, the adopted atomic parameters for each line are also of paramount importance. Although we can find very accurate wavelengths and excitation potentials for each line, the oscillator strengths ( $\log gf$ ) are not so precisely known. The uncertainties of these values, which can be measured in laboratory, can propagate and affect dramatically the precision and accuracy of the derived spectroscopic parameters.

## 2.2 Measurement of EWs

Although the definition of the an EW is quite simple, its measurement from an observed spectra can still be tricky (second step). The **determination of the correct position of the continuum level** continues to be an important source for the uncertainties in these measurements. Another important aspect is to understand if a given

line that needs to be measured is completely isolated (the ideal case) or if there are close-by lines that are blended together. In the latter case the correct identification of all lines is fundamental for a good measurement.

Moreover, for the EW measurements is important to define the profile function used for the line fit and corresponding strength calculation of each lines. The Gaussian profile is widely used and is considered to be an almost perfect approximation for weak absorption lines. However some caution should be taken when measuring strong lines (typically  $EW > 150 \text{ mÅ}$ ). In this case the Gaussian profile cannot perfectly fit the wings of the line. In these cases several authors prefer to use the Lorentzian profile.

Until recently, these measurements were only feasible using interactive routines such as the “splot” task in IRAF<sup>1</sup>. In this case, people have to go through the spectrum line by line, marking the continuum position by eye and make the EW measurement. This is, of course, a quite boring and very time consuming task. Even worse, the subjectivity involved in such interactive routines may lead to inconsistency between the measurements of different lines. To overcome this issues, several automatic codes are now on the market (e.g. ARES, Sousa et al. (2007); DAOSPEC, Stetson et al. (2008)) that measure the EWs in a more efficient and consistent way.

### 2.3 Model Atmospheres

The literature offers the possibility to choose from a wide variety of model atmospheres (third step) and often this choice can be affected by subjectivity. Models like ATLAS9 (Kurucz et al. , 1993) and MARCS (Gustafsson et al. , 2008) stand out as the most used set of atmospheric models for the derivation of spectroscopic and elemental abundances.

The way the models are created and used in each method can also differ. Some authors prefer to create the models on the spot making use of available codes. As an alternative, and in order to increase the efficiency of each method, grids are created with pre-computed model atmospheres, which can be directly selected for each step of the iteration, or instead, the grid of models can be used for interpolations allowing this way a better refinement in the search of the “final” stellar parameters.

As one could expect, for the creation of the models there are a series of important physical parameters and approximations that need to be defined and used for the correspondent computation. For instance, for FGK solar-type stars the plane-parallel approximation has been proved to be a safe approach, but specific models may be necessary when dealing with “special” types of stars (e.g., metal-poor stars, giant and evolved stars).

---

<sup>1</sup> IRAF is distributed by National Optical Astronomy Observatories, operated by the Association of Universities for Research in Astronomy, Inc., under contract with the National Science Foundation, USA

## 2.4 Computing Abundances

In step number four we have the **computation of the iron abundance** (or any other chemical element). This step clearly depends on the measured strength of the line as well as the selection of the atmospheric model.

As for such models, **local thermodynamical equilibrium (LTE) is commonly assumed as a valid approximation for FGK solar-type stars**. However, this approximation may not be completely valid for other types of stars (e.g., for very metal-poor stars NLTE corrections may be necessary to apply (Bergemann et al. , 2012).

## 2.5 Finding the correct parameters

In step five we need to achieve the excitation and ionization equilibria. The correlation between the excitation potential and the iron abundance of each line constrains the effective temperature, the correlation between the reduced equivalent width and the individual abundance constrains the microturbulence, and the ionization balance between the mean abundance of FeI and FeII fixes the surface gravity. The "final" stellar parameters will be obtained when no correlations are present, i.e. when all lines give the same individual abundances we stop the process and keep the parameters from the adopted model atmosphere. The iron abundance comes as an additional result from this analysis and is taken as the mean abundance from all lines.

The main difference between the various EW methods in this step may be related with the way in which the parameters are found and constrained. There are different minimization algorithms that may be used to explore the parameter space and the respective inter-dependences. Finally the constraints used to stop the method and check for the correct convergence of the parameters (i.e. what is the definition of no correlation from the data, e.g. does a slope with a value of 0.01 represents no correlation?) are crucial for the final decision of each method that may change the resulting parameters.

## 3 ARES+MOOG: the method

So far it was described a general overview of an EW method. Here we will go through the steps once again and describe the specific choices made in the ARES+MOOG (whose workflow is described in Fig. 1).

### 3.1 Line list

Since this method was designed to be completely automatic, for the compilation of the line list we have **selected as many lines as possible**. This **increases the statistical strength of the derived parameters**. However, each line was carefully selected in order to be **considered stable** for this method (for further details on the stability of the lines see Sousa et al. , 2008).

Regarding the atomic data, in order to overcome the uncertainties for the  $\log gf$  described before, we made use of a differential analysis technique. This technique consists in selecting a benchmark star (typically the Sun) with very well constrained parameters. The goal of this analysis is to recompute the  $\log gf$  using an inverse analysis. We first measured EWs for our selected lines in the solar spectrum. Then, assuming the solar parameters (e.g.  $T_{\text{eff}} = 5777\text{K}$ ,  $\log g = 4.44$  dex,  $\xi_t = 1.00 \text{ km s}^{-1}$ , and  $\log(\text{Fe}) = 7.47$ ), the values for each  $\log gf$  were then changed until we derive the "correct" individual abundance for each line.

Using this differential analysis it is possible to reduce both the errors on the atomic parameters and the errors on measurements of the equivalent widths. When measuring the lines in a benchmark star we are also including errors given by its spectrum itself. For instance, the existence of small undetected blended lines or the intrinsic bad position of the continuum for each line will introduce errors when computing the  $\log gf$ . The differential analysis will allow us to partially compensate for such kind of errors by assuming a systematic measurement of the EW for the same lines of the stars analyzed. An obvious drawback from this analysis is that the results strongly deteriorate as we use the  $\log gf$  in stars that become more and more different from the benchmark star.

### 3.2 Measuring EWs

The Equivalent Width of the lines were automatically determined using ARES<sup>2</sup> code (Sousa et al. , 2007) following the approach of Sousa et al. (2008) and Sousa et al. (2011) to adjust the *rej* parameter of ARES according to the  $S/N$  of each spectrum. In the next section the input parameters for ARES will be described in detail and some advices will be given in order to select the best input parameters.

### 3.3 Model Atmospheres

We used MOOG 2013<sup>3</sup> (Snedden , 1973) to compute the line-by-line abundance for each star assuming LTE conditions. In our standard method we used a grid of Kurucz

---

<sup>2</sup> The ARES code can be downloaded at <http://www.astro.up.pt/~sousasag/ares/>

<sup>3</sup> <http://www.as.utexas.edu/~chris/moog.html>

Atlas 9 plane-parallel model atmospheres (Kurucz et al. , 1993) in order to generate the appropriate model atmosphere through interpolation. This model is then feed as an input into MOOG to compute the abundances through the driver *abfind*.

### 3.4 Finding the final parameters and the Iron Abundance

We use as minimization algorithm to determinate the best stellar parameters the Downhill Simplex Method (Press et al. , 1992). Moreover, in order to identify outliers caused by incorrect EW values, we performed a  $3\text{-}\sigma$  clipping for the FeI and FeII lines after a first preliminary determination of the stellar parameters. After this, the procedure was executed once again without the rejected lines. For a wider discussion about the full automatization of this method see the works of Santos (2004); Sousa et al. (2011); Saffe (2011).

## 4 ARES+MOOG: Quick Tutorial

The tutorial presented here follows the procedures and codes that were made available at the “Spring School of Spectroscopic Data Analyses”. The codes are available either at the respective web-pages or are still accessible from the school web-page: <http://spectra.astro.uni.wroc.pl/>.

As described before, the first step for the ARES+MOOG method is the definition of the line list. We will use the very well defined line list composed of nearly 300 iron lines presented in Sousa et al. (2008). If the reader is interested in a recent update of the line list see Tsantaki et al. (2013).

### 4.1 Using ARES

A complete description of ARES can be found in Sousa et al. (2007). In this document we will only point out the essential steps required to properly run the code.

A sketch of the ARES procedure is presented in Figure 1 of Sousa et al. (2007). The basic steps of ARES are: i) the reading of both the spectrum and the line list; ii) the local normalization of the spectrum which is performed for each line in each iteration; iii) the detection of the set of lines that are needed to be fitted (in case of blended lines); iv) the fit and the measurement of the EWs; v) the storage of the EWs in an output file.

#### 4.1.1 Preparing the spectrum

The first step to properly use ARES is the **preparation of the observed spectra**. The available version of ARES only works with one-dimensional FITS spectrum. In the respective FITS header of the spectrum the CDEL1 and CRVAL1 keywords need to be defined as a requirement.

Another fundamental condition is that the spectrum should be **corrected in radial velocity** so that the absorption lines are found at the rest frame, otherwise ARES will not be able to find the correct line position for the analysis.

#### 4.1.2 The line list

The only requirement for the line list to be feed in ARES is the correct wavelength. The file with the list of lines should consist of a column with the wavelength. ARES will read this file line-by-line for the respective EW measurement. It may be also useful to keep in this file the atomic data for each line that will be required later on. In Table 1 is presented a sample of line list from (Sousa et al. , 2008), where for each line is defined the rest wavelength ( $\lambda$ ), the excitation potential ( $\chi_i$ ), the oscillator strength( $\log gf$ ) the element identification (Ele. and Num.) and the EW measured in a solar spectrum ( $EW_{\odot}$ ).

**Table 1** Sample of the line-list presented in (Sousa et al. , 2008).

$\lambda$ (Å)	$\chi_i$	$\log gf$	Ele.	Num.	$EW_{\odot}$
6079.01	4.65	-1.008	FeI	26.0	45.8
6082.72	2.22	-3.566	FeI	26.0	34.5
6084.11	3.20	-3.774	FeII	26.1	20.9
6089.57	4.58	-1.273	FeI	26.0	35.3
...	...	...	...	...	...

#### 4.1.3 ARES input parameters

The input parameters for ARES are the following:

- *specfits*: The name of the 1D fits file with the spectrum corrected in Radial Velocity (e.g. HD1234\_rv.fits).
- *readlinedat*: The name of the file with the list of lines to be measured (e.g. line list.dat).
- *fileout*: The name of the file that will contain the output of the results (e.g. HD1234.ares).
- *lambdai*: Initial wavelength to search the lines (e.g. 3000 Å).
- *lambdaf*: Final wavelength to search the lines (e.g. 7000 Å).



- **smoothder**: Smooth value for the derivatives that are used for the line detection procedure (e.g. 4 - recommended value for high resolution spectra and good S/N).
- **space**: Size of the local spectrum interval in Angstroms around each line. Only this interval is used for the individual computations of each line (e.g. 3 Å- recommended value).
- **rejt**: Parameter for the calibration of the continuum position. This value strongly depends on the S/N of the spectrum. A good reference for the values to be used here can be found in Sousa et al. (2008, 2011) (e.g. 0.996 for spectra with S/N  $\sim 400$ ).
- **lineresol**: This parameter sets the line resolution of the input spectra; This parameter is helpful to distinguish real lines from noise (e.g. 0.1 Å- recommended value for high resolution spectra).
- **miniline**: Lines with strength weaker than this value are not printed in the output file (e.g. 2 mÅ).
- **plots\_flag**: Flag for the plots (0-runs in batch, 1-shows the plots and stops for each line calculation).

There are specific input parameters that are very important to obtain correct EWs. A proper selection of the **rejt** parameter is fundamental in order to track the correct continuum position. Wrong values of this parameter may systematically give larger (or smaller) EWs. Although there is a clear dependence between this parameter and the S/N we choose to leave this as a free parameter given the high degree of subjectivity when defining the continuum position. If some authors want to define their own S/N dependence, we advise the reader to select only a few isolated lines for a few spectra with different S/N and to make use of the plots to select the best values for each S/N. For more details on such exercise see the work of Mortier et al. (2013). For the other parameters, the recommended values should be kept fixed. We may only consider to tweak the **smoothder** parameter at higher values in case of very low S/N spectra. This may help for the correct identification of real lines in noisy spectra.

## 4.2 Generating a model atmosphere

The computations of specific model atmospheres in ARES+MOOG is done by an interpolation code which in turn uses a grid of pre-computed ATLAS9 models. The interpolation of models was chosen here for efficiency purposes and consists in of two separated Fortran codes: the first code performs the interpolation itself, while the second one accommodates the model in a file with a specific format readable by MOOG. A script named “make\_model.bash”<sup>4</sup> is provided in order to run both codes directly. The script needs as input the astrophysical parameters ( $T_{\text{eff}}$ ,  $\log g$ ,  $\xi$ , and [Fe/H]) to generate the model which will be stored in a file named “out.atm”.

<sup>4</sup> This script can be found together with other codes used in the school in: [http://spectra.astro.uni.wroc.pl/elements/codes\\_ARESMOOG.tar](http://spectra.astro.uni.wroc.pl/elements/codes_ARESMOOG.tar)

### 4.3 Using MOOG

MOOG is a code that performs a variety of LTE line analysis and spectrum synthesis tasks. The **typical use of MOOG is to assist in the determination of the chemical composition of a star**. In our case we want to measure individual iron line abundances to derive the stellar parameters.

There are several drivers available to run MOOG for several different purposes. The MOOG user's manual has a complete description of the several drivers. For ARES+MOOG we make use of the *abfind* driver.

One of the chief assets of MOOG is its ability to do on-line graphics. However in ARES+MOOG the graphics are not used at all. The visualization of different plots is quite useful to see the dependences of the different parameters with the individual abundance determination. Together with a modified MOOG version (where the internal plots were ignored since it requires a proprietary library), it was provided a simple Python code to perform the plots (named `read_moog_plot.py`)<sup>4</sup>. This code is used to illustrate the parameters dependences and respective correlations (see the next sections).

Another important input for MOOG is the list of atomic data for each line in order to perform individual abundance calculations. For this purpose, an additional script was provided (`make_linelist_local.bash`)<sup>4</sup>; this script reads the output of ARES and the initial line list to create the required format file for MOOG.

### 4.4 Search for the correct model

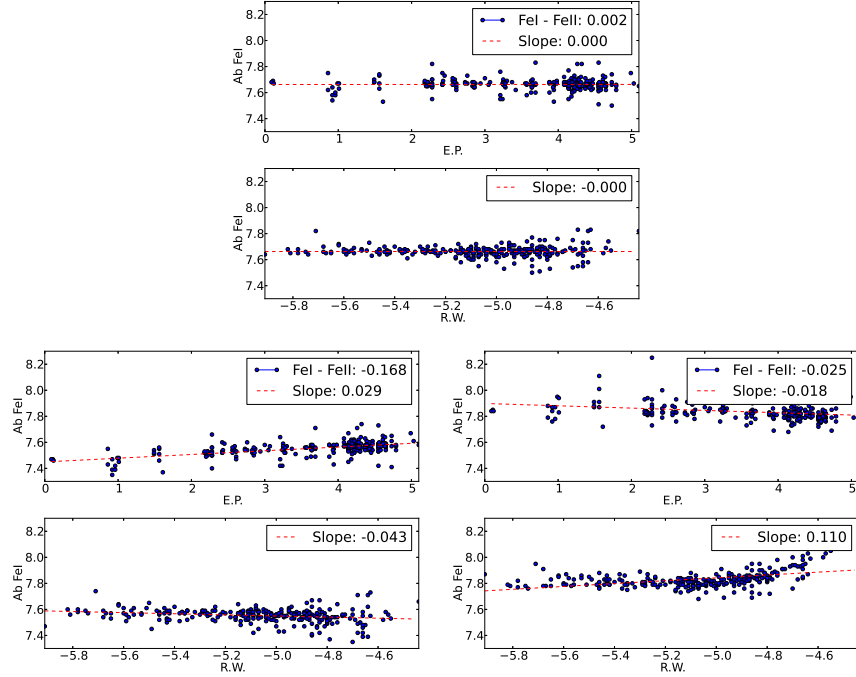
For this tutorial we will make use of the solar type star HD1461 for which an HARPS-S@La Silla spectrum with high resolution and high S/N was analysed by Sousa et al. (2008). The final parameters derived for this star and obtained by the authors with ARES+MOOG are:  $T_{\text{eff}} = 5765 \pm 18$  K,  $\log g = 4.38 \pm 0.03$  dex, a  $\xi = 0.97 \pm 0.02$  Km/s, and  $[Fe/H] = 0.19 \pm 0.01$  dex<sup>5</sup>.

Fig. 2 shows the correlations between the iron abundance ( $\text{Ab(FeI)}$ ) and the excitation potential (E.P.) and the reduced equivalent width (R.W.) for all the used iron lines of HD1461. In the same figure it is also indicated together with the respective slopes of the correlations, the difference between the average abundances of FeI and FeII ( $\langle \text{Ab(FeI)} \rangle - \langle \text{Ab(FeII)} \rangle$ ). From the values indicated in the figure we can see that the slopes of the correlations obtained with the "final" stellar parameters are close to zero, as well as the difference between FeI and FeII.

From theoretical studies, it is possible to demonstrate the the  $T_{\text{eff}}$  has a strong influence in the correlation  $\text{Ab(FeI)}$  vs. E.P., the microturbulence in the correlation  $\text{AB(FeI)}$  vs. R.W., and the surface gravity is connected directly with  $\langle \text{Ab(FeI)} \rangle - \langle \text{Ab(FeII)} \rangle$  (see, e.g. Gray, David F. , 2005). Therefore, here in the following,

---

<sup>5</sup> For a proper description on the estimation of the errors with the ARES+MOOG method, see Sousa et al. (2011)



**Fig. 2** Abundance of FeI as a function of excitation potential (E.P.) and reduced wavelength (R.W.). The top panel shows the result for the “final” stellar parameters, while in the bottom panels the temperature was changed to a lower value (5600 K; left panel), and to an upper value (5900 K; right panel).

we will make a series of exercises with the aim to show the dependence of each correlation with the spectroscopic parameters, and to illustrate how the “final” stellar parameters were derived for HD1461. In particular, we will show these dependences in a practical way making use of the codes provided for the ARES+MOOG method.

#### 4.4.1 Effective temperature dependence

The lower panels of Fig. 2 show the computed abundances for a model with exactly the same parameters as the final ones with exception of the temperature. It is clear that the slopes of the correlations change dramatically. Not only the Ab(FeI) vs. E.P. changes but also the same happens for Ab(FeI) vs. R.W. showing that the stellar parameters are strongly inter-dependent.

Hence, these plots show how Ab(FeI) vs. E.P. varies with the changes in temperature so we can react accordingly to find the correct temperature. In particular, when we underestimate the temperature the slope is positive, while when we overes-

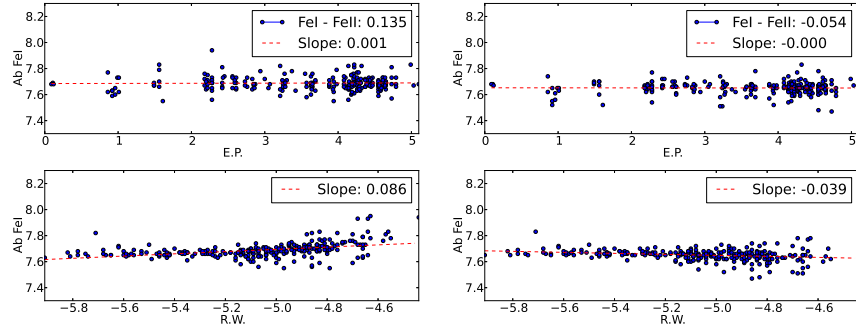


**Fig. 3** Same as Fig. 2 but instead of changing the temperature, here we changed the surface gravity to a lower value (4.10 dex; left panel), and an upper value (4.50 dex; right panel).

timize the real temperature, the slope becomes negative. Therefore, the slope gives us information about the direction where the correct temperature is.

#### 4.4.2 Surface Gravity dependence

A similar exercise can be done for the surface gravity. Here the temperature was set back to its “final” value and only the gravity was changed to observe how  $\langle \text{Ab}(\text{FeI}) \rangle - \langle \text{Ab}(\text{FeII}) \rangle$  varies accordingly. Figure 3 shows the results. In particular, when we underestimate the surface gravity  $\langle \text{Ab}(\text{FeI}) \rangle - \langle \text{Ab}(\text{FeII}) \rangle$  is positive, while when we overestimate the surface gravity the  $\langle \text{Ab}(\text{FeI}) \rangle - \langle \text{Ab}(\text{FeII}) \rangle$  is negative.

One interesting fact is that the changes on the surface gravity nearly does not affect  $\text{Ab}(\text{FeI})$  vs. E.P. (see Fig. 3). This means that the  $\log g$  derived through this method is almost independent on the temperature, and vice-versa. This is certainly an advantage of this method showing that the temperature and the iron abundance are independently well constrained. A clear disadvantage here is that the  $\log g$  is not very well constrained, due to the reduced number of ionized iron lines compared to FeI lines. This means that extra caution should be considered for the derived values of the surface gravity. For more details on this issue see the work of Torres et al. (2012).

#### 4.4.3 Microturbulence dependence

A final exercise can be made for the microturbulence. Again all parameters are set to the “final” values with the exception of the adopted microturbulence. This parameter is connected with the saturation of the stronger iron lines. A good value for the

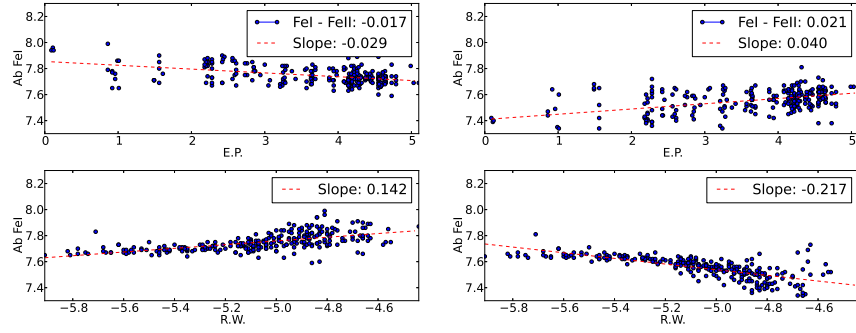


**Fig. 4** Same as Fig. 2 but instead of changing temperature, here we change the microturbulence to a lower value (0.5 km/s; left panel), and an upper value (1.5 km/s; right panel) than the final  $\xi$ .

microturbulence will allow us to derive the same abundances for weak and strong iron lines.

The left panel of Fig. 4 shows the result of the abundances when the microturbulence is underestimated. The slope of  $\text{Ab}(\text{FeI})$  vs.  $\text{R.W.}$  is positive in this case. This means that the “final” value for the microturbulence should be higher. The opposite happens when we overestimate the microturbulence, as can be seen from the right panel of Fig. 4.

#### 4.4.4 Final Remark

Finally, an additional detail regarding the model atmosphere should be considered. When the final parameters are derived, the resulting iron abundance (derived from the average of the measured line equivalent widths) must be compatible with the metallicity of the model atmosphere.

## 5 Summary

In this document we described in practical terms the use of the EW method to derive spectroscopic stellar parameters. We made a general overview of the several steps required to use this method. We described several options used by different authors, namely the use of different line lists, and model atmospheres.

The ARES+MOOG method was described in some detail where we tried to give the best advices for a proper use of it, especially in what regards the use of the ARES code to automatically compute the equivalent widths.

The details on how the method finds the “final” set of stellar parameters are exposed here. From the practical point of view, the essential steps of the method are

described and can be used as a guideline for future works. Some additional points to fully complete the description of ARES+MOOG were left a side. These include the minimization algorithm which allows a proper automatization of the full process and the estimation of the uncertainties.

**Acknowledgements** S.G.S acknowledges the support from the Fundação para a Ciência e Tecnologia (Portugal) and FSE/POPH in the form of the grants SFRH/BPD/47611/2008 and the scientific cooperation project FCT/Poland 2011/2012 (Proc. 441.00 Poland). S.G.S also acknowledges the support by the European Research Council/European Community under the FP7 through a Starting Grant (ERC-2009-StG-239953).

## References

- Bergemann, M.; Lind, K.; Collet, R., et al. 2012, MNRAS, 427, 1, 27
- Gray, David F. 1995, The Observation and Analysis of Stellar Photospheres, 3rd Edition
- Gustafsson, B., Edvardsson, B., Eriksson, K., et al. 2008, A&A, 486, 951
- Kurucz, R. 1993, ATLAS9 Stellar Atmosphere Programs and 2 km/s grid. Kurucz CD-ROM No. 13. Cambridge, Mass.: Smithsonian Astrophysical Observatory, 1993., 13
- Mortier, A., Santos, N. C., Sousa, S. G., et al. 2013, A&A, 557, A70
- Press, W. H., Teukolsky, S. A., Vetterling, W. T., & Flannery, B. P. 1992, Cambridge: University Press, 1992, 2nd ed.,
- Saffe, C., Revista Mexicana de Astronomia y Astrofisica Vol. 47, pp. 3-14 (2011)
- Santos, N. C.; Israelian, G.; Mayor, M., A&A, 415, 1153
- Snedden, C. A. 1973, Ph.D. Thesis,
- Sousa, S. G., Santos, N. C., Israelian, G., Mayor, M., & Monteiro, M. J. P. F. G. 2007, A&A, 469, 783
- Sousa, S. G., Santos, N. C., Mayor, M., et al. 2008, A&A, 487, 373
- Sousa, S. G., Santos, N. C., Israelian, G., et al. 2011, A&A, 526, id.A99
- Sousa, S. G., Santos, N. C., Israelian, G., et al. 2011, A&A, 533, id.A141
- Stetson, P. B. & Pancino, E. 2008, PASP, 120, 1332
- Torres, G., Fischer, D. A., Sozzetti, A., et al. 2012, APJ, 757, 2, 161, 14
- Tsantaki, M., Sousa, S. G., Adibekyan, V. Zh., et al. 2013, A&A, 555, A150